Measurement of Angular and CP Asymmetries in D[superscript 0] → π[superscript +]π[superscript −]μ[superscript +]μ[superscrpt −] and D[superscript 0] → K[superscript +]K[superscript −] μ[superscript +] μ[superscript −] Decays

Measurement of Angular and *CP* Asymmetries in $D^0 \to \pi^+\pi^-\mu^+\mu^-$ and $D^0 \to K^+K^-\mu^+\mu^-$ Decays

R. Aaij *et al.*[*]
(LHCb Collaboration)

(Received 28 June 2018; published 30 August 2018)

The first measurements of the forward-backward asymmetry of the dimuon pair ($A_{\rm FB}$), the triple-product asymmetry ($A_{2\phi}$), and the charge-parity-conjugation asymmetry (A_{CP}), in $D^0 \to \pi^+\pi^-\mu^+\mu^-$ and $D^0 \to K^+K^-\mu^+\mu^-$ decays are reported. They are performed using data from proton-proton collisions collected with the LHCb experiment from 2011 to 2016, corresponding to a total integrated luminosity of 5 fb^{-1}. The asymmetries are measured to be $A_{\rm FB}(D^0 \to \pi^+\pi^-\mu^+\mu^-) = (3.3 \pm 3.7 \pm 0.6)\%$, $A_{2\phi}(D^0 \to \pi^+\pi^-\mu^+\mu^-) = (-0.6 \pm 3.7 \pm 0.6)\%$, $A_{CP}(D^0 \to \pi^+\pi^-\mu^+\mu^-) = (4.9 \pm 3.8 \pm 0.7)\%$, $A_{\rm FB}(D^0 \to K^+K^-\mu^+\mu^-) = (0 \pm 11 \pm 2)\%$, $A_{2\phi}(D^0 \to K^+K^-\mu^+\mu^-) = (9 \pm 11 \pm 1)\%$, $A_{CP}(D^0 \to K^+K^-\mu^+\mu^-) = (0 \pm 11 \pm 2)\%$, where the first uncertainty is statistical and the second systematic. The asymmetries are also measured as a function of the dimuon invariant mass. The results are consistent with the standard model predictions.

DOI: 10.1103/PhysRevLett.121.091801

Decays of charm hadrons into final states containing muon pairs may proceed via the so-called *short-distance* $c \to u\mu^+\mu^-$ flavor-changing neutral-current process. In the standard model (SM) such process can only occur through electroweak loop transitions that are highly suppressed by the Glashow-Iliopoulos-Maiani mechanism [1]. The short-distance contribution to the inclusive $D \to X\mu^+\mu^-$ branching fraction, where X represents one or more hadrons, is predicted to be $\mathcal{O}(10^{-9})$ [2]. The branching fraction can be greatly enhanced if new particles are exchanged in the loop, making these decays interesting for searches for physics beyond the SM. However, the SM branching fraction can increase up to $\mathcal{O}(10^{-6})$ [2–5] because of *long-distance* contributions occurring through tree-level amplitudes involving intermediate resonances that subsequently decay into $\mu^+\mu^-$. Hence, the sensitivity to the short-distance amplitudes is greatest for dimuon masses away from the peaks of the resonances, although resonances populate the entire dimuon-mass spectrum due to their long tails. Additional discrimination between short- and long-distance contributions can be obtained by studying kinematic correlations between final-state particles of multibody decays and charge-parity (CP) conjugation asymmetries. These asymmetries are predicted to be negligibly small in the SM but could be as large as $\mathcal{O}(1\%)$ in scenarios of physics beyond the SM [4–11].

The semileptonic four-body decays $D^0 \to h^+h^-\mu^+\mu^-$ (charge-conjugated decays are implied unless stated otherwise), where h is either a pion or a kaon, are described by five independent kinematic variables (Fig. 1): the dimuon invariant mass, $m(\mu^+\mu^-)$, the dihadron invariant mass, $m(h^+h^-)$. the angle θ_μ between the μ^+ (μ^-) direction and the direction opposite to the D^0 ($\bar{D}^0$) meson in the dimuon rest frame, the angle θ_h between the h^+ (h^-) direction and the direction opposite to the D^0 ($\bar{D}^0$) meson in the dihadron rest frame, and the angle ϕ between the two planes formed by the dimuon and the dihadron systems in the rest frame of the D^0 meson (the angle ϕ is zero if the two planes are parallel). Among all the possible angular observables that can be constructed, the forward-backward asymmetry of the dimuon system,

$$A_{\rm FB} = \frac{\Gamma(\cos\theta_\mu > 0) - \Gamma(\cos\theta_\mu < 0)}{\Gamma(\cos\theta_\mu > 0) + \Gamma(\cos\theta_\mu < 0)}, \tag{1}$$

and the triple-product asymmetry,

$$A_{2\phi} = \frac{\Gamma(\sin 2\phi > 0) - \Gamma(\sin 2\phi < 0)}{\Gamma(\sin 2\phi > 0) + \Gamma(\sin 2\phi < 0)}, \tag{2}$$

together with the CP asymmetry,

$$A_{CP} = \frac{\Gamma(D^0 \to h^+h^-\mu^+\mu^-) - \Gamma(\bar{D}^0 \to h^+h^-\mu^+\mu^-)}{\Gamma(D^0 \to h^+h^-\mu^+\mu^-) + \Gamma(\bar{D}^0 \to h^+h^-\mu^+\mu^-)}, \tag{3}$$

[*]Full author list given at the end of the Letter.

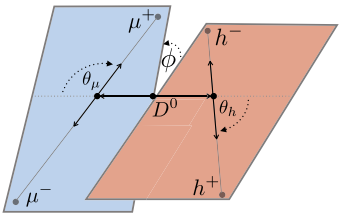

FIG. 1. Diagram showing the topology of a $D^0 \to h^+h^-\mu^+\mu^-$ decay, with the definition of the angles that are relevant for the measurement.

are considered to be promising probes for physics beyond the SM [4,5].

The $D^0 \to \pi^+\pi^-\mu^+\mu^-$ and $D^0 \to K^+K^-\mu^+\mu^-$ decays have been recently observed by the LHCb Collaboration [12] and their branching fractions have been measured to be $(9.6 \pm 1.2) \times 10^{-7}$ and $(1.54 \pm 0.33) \times 10^{-7}$, respectively, in agreement with SM predictions [4,5]. However, angular and CP asymmetries are yet to be measured.

This Letter reports the first measurement of $A_{\rm FB}$, $A_{2\phi}$, and A_{CP} in $D^0 \to \pi^+\pi^-\mu^+\mu^-$ and $D^0 \to K^+K^-\mu^+\mu^-$ decays using $p\ p$ collision data collected with the LHCb experiment at center-of-mass energies of 7, 8, and 13 TeV between 2011 and 2016. The combined data set corresponds to a total integrated luminosity of 5 fb^{-1}. The analysis is performed using D^0 mesons originating from $D^{*+} \to D^0\pi^+$ decays, with the D^{*+} meson produced at the primary $p\ p$ collision vertex. The charge of the pion from the $D^{*\pm}$ decay determines the flavor of the neutral D meson at production. The signal is studied in regions of dimuon mass defined according to the known resonances as in Ref. [12]. The regions dominated by the ρ^0/ω and the ϕ resonances are further split in two around the resonance mass to account for a possible variation of the asymmetries across the resonance [5,9,11]. For $D^0 \to \pi^+\pi^-\mu^+\mu^-$ decays the regions are (low-mass) < 525 MeV$/c^2$, (η) 525–565 MeV$/c^2$, (ρ^0/ω-low) 565–780 MeV$/c^2$, (ρ^0/ω-high) 780–950 MeV$/c^2$, (ϕ-low) 950–1020 MeV$/c^2$, (ϕ-high) 1020–1100 MeV$/c^2$, and (high-mass) > 1100 MeV$/c^2$. The same regions are considered for $D^0 \to K^+K^-\mu^+\mu^-$ decays, except for the ρ^0/ω region, which is not split in two because of the reduced size of this sample, and the ϕ and high-mass regions, which are not kinematically accessible. The asymmetries are determined only in $m(\mu^+\mu^-)$ regions where a significant signal yield was previously observed [12]. No measurement is performed in the η region of both channels and in the high-mass region of $D^0 \to \pi^+\pi^-\mu^+\mu^-$. Furthermore, to avoid potential experimenter's bias on the measured quantities, all asymmetries were shifted by an unknown value during the development of the analysis and examined only after the analysis procedure was finalized.

The LHCb detector [13,14] is a single-arm forward spectrometer designed for the study of particles containing b or c quarks. It includes a high-precision tracking system consisting of a silicon-strip vertex detector surrounding the $p\ p$ interaction region, a large-area silicon-strip detector located upstream of a dipole magnet with a bending power of about 4 Tm, and three stations of silicon-strip detectors and straw drift tubes placed downstream of the magnet. The polarity of the magnetic field is reversed periodically throughout the data-taking. Particle identification is provided by two ring-imaging Cherenkov detectors, an electromagnetic and a hadronic calorimeter, and a muon system composed of alternating layers of iron and multiwire proportional chambers. Events are selected online by a trigger that consists of a hardware stage, which is based on information from the calorimeter and muon systems, followed by a software stage, based on information on charged tracks in the event that are displaced from any primary vertex. A subsequent software trigger exploits a full event reconstruction [15] to exclusively select $D^0 \to h^+h^-\mu^+\mu^-$ decays. Candidate D^0 mesons are constructed by combining four charged tracks, each having momentum $p > 3$ GeV$/c$ and transverse momentum $p_{\rm T} > 0.5$ GeV$/c$, that form a secondary vertex separated from any primary vertex in the event. Two oppositely charged particles are required to be identified as muons.

The D^0 candidates satisfying the trigger requirements are further selected through particle-identification criteria placed on their decay products. Candidates with an invariant mass $m(h^+h^-\mu^+\mu^-)$ in the range 1810–1940 MeV$/c^2$ are then combined with a charged particle originating from the same primary vertex and having $p_{\rm T} > 120$ MeV$/c$, hereafter referred to as soft pion, to form a $D^{*+} \to D^0\pi^+$ decay candidate. When more than one primary vertex is reconstructed, the one with respect to which the D^0 candidate has the lowest impact-parameter significance is chosen. The vertex formed by the D^0 and π^+ mesons is constrained to coincide with the primary vertex and the difference between the D^{*+} and D^0 masses, Δm, is required to be in the range 144.5–146.5 MeV$/c^2$ (corresponding to approximately $\pm 3\sigma$ in mass resolution around the signal peak). A fiducial-region requirement is implemented to reduce instrumental charge asymmetries that can bias the A_{CP} measurement. The fiducial region restricts the soft-pion trajectory to be within a fully instrumented region of the detector, because particles near the edge of the detector acceptance have different efficiencies to be reconstructed depending on their charge and the magnet polarity [16].

A multivariate selection, based on a boosted decision tree (BDT) [17,18] with gradient boosting [19], is then used to suppress background from combinations of charged particles not originating from a D^{*+} decay. The features used in the BDT to discriminate signal from this *combinatorial* background are: the momentum and transverse momentum of the soft pion, the smallest impact parameter of the D^0 decay products with respect to the primary vertex, the

angle between the D^0 momentum and the vector connecting the primary and secondary vertices, the quality of the secondary vertex, its separation from the primary vertex, and a measure of the isolation of the D^{*+} candidate from other tracks in the event. The BDT is trained separately for $D^0 \to \pi^+\pi^-\mu^+\mu^-$ and $D^0 \to K^+K^-\mu^+\mu^-$ decays, because of their different kinematic properties, using simulated decays as signal and data candidates with $m(h^+h^-\mu^+\mu^-)$ between 1890 and 1940 MeV/c^2 as background. A detailed description of the LHCb simulation can be found in Refs. [20,21]. To minimize biases on the background classification, the training samples are further randomly split in two disjoint subsets. The classifier trained on one subset is applied to the other, and vice versa.

The largest source of specific background is due to the hadronic four-body decays $D^0 \to \pi^+\pi^-\pi^+\pi^-$ and $D^0 \to K^+K^-\pi^+\pi^-$, where two pions are misidentified as muons. The misidentification occurs mainly when the pions decay in flight into a muon and an undetected neutrino. This background is suppressed by a multivariate muon-identification discriminant that combines the information from the Cherenkov detectors, the calorimeters and the muon system [22,23]. Thresholds on the BDT response and on the muon-identification discriminant are optimized simultaneously by minimizing the statistical uncertainty on the measured asymmetry, as determined in data from randomly tagged D^0 and $\bar{D}^0$ candidates. After selection, less than 1% of the events contain multiple candidates that share final-state particles. In these events one candidate is selected at random. The final samples comprise 1326 ± 45 $D^0 \to \pi^+\pi^-\mu^+\mu^-$ and 137 ± 14 $D^0 \to K^+K^-\mu^+\mu^-$ signal decays, as determined from fits to the $m(h^+h^-\mu^+\mu^-)$ distributions.

The selected candidates are corrected for any distortion of the phase space caused by the reconstruction and selection criteria. The efficiency for reconstruction and selection is modeled across the full five-dimensional phase space. This is achieved by using a BDT with gradient boosting [17–19] as a classification tool that learns about the different features of the generated and selected samples and combines them into a single variable [24]. A weight corresponding to the inverse of the per-candidate efficiency is then computed as the ratio between the predicted probabilities for selected and generated candidates as a function of the BDT response. The training of this *weighting* BDT is performed on simulated events before and after selection, using $|\cos\theta_\mu|$, $|\cos\theta_h|$, $m(h^+h^-)$ and $m(\mu^+\mu^-)$ as input variables. This choice is justified by the observation that the efficiency is symmetric with respect to the angular variables, that it does not depend on $\sin 2\phi$, and that $\sin 2\phi$ is not correlated with any other variable. As a consequence of the efficiency weighting, the effective sample size of the $D^0 \to \pi^+\pi^-\mu^+\mu^-$ ($D^0 \to K^+K^-\mu^+\mu^-$) sample is reduced by about 13% (14%).

The CP-asymmetry measurement is affected by $\mathcal{O}(1\%)$ nuisance charge asymmetries introduced by the different efficiency to reconstruct a positively or negatively charged soft pion, $A_D(\pi^+)$, and the different production cross sections of D^{*+} and D^{*-} mesons, $A_P(D^{*+})$. For small asymmetries, the *raw* asymmetry between observed yields of $D^{*+} \to D^0(\to f)\pi^+$ and $D^{*-} \to \bar{D}^0(\to f)\pi^-$ decays, where f is a CP-symmetric final state, can be approximated as $A_{CP}^{\rm raw}(f) \approx A_{CP}(f) + A_P(D^{*+}) + A_D(\pi^+)$. The nuisance charge asymmetries are subtracted from the raw asymmetry using high-yield samples of $D^{*+} \to D^0(\to K^+K^-)\pi^+$ decays. Therefore, CP asymmetry is given by $A_{CP}(h^+h^-\mu^+\mu^-) = A_{CP}^{\rm raw}(h^+h^-\mu^+\mu^-) - A_{CP}^{\rm raw}(K^+K^-) + A_{CP}(K^+K^-)$, where $A_{CP}(K^+K^-) = (-0.06 \pm 0.18)\%$ is taken from the independent measurement of Ref. [25]. To account for different kinematic distributions in the signal and control modes, the procedure is performed in disjoint ranges of transverse and longitudinal momentum of the D^{*+} candidate.

The asymmetries $A_{\rm FB}$, $A_{2\phi}$, and A_{CP} of the signal decays are determined through unbinned maximum-likelihood fits to the $m(h^+h^-\mu^+\mu^-)$ distributions of the selected candidates, weighted with the inverse of the per-candidate phase-space-dependent efficiency. The data are split into different tag categories (defined by the sign of $\cos\theta_\mu$, the sign of $\sin 2\phi$ or the soft-pion charge) and a simultaneous fit is performed on the obtained data sets with the asymmetries as free parameters. The data are described by the sum of three components: the signal, the misidentified background, and the combinatorial background. Analogously to Ref. [12] the signal is described with a Johnson's S_U distribution [26] with parameters determined from simulation. The mass shape of the misidentified background is determined using separate data samples of $D^0 \to h^+h^{(\prime)-}\pi^+\pi^-$ decays where the D^0 mass is calculated assigning the muon-mass hypothesis to two oppositely charged pions. The combinatorial background is described by an exponential function. The shape of this background is fixed from data candidates with Δm above 150 MeV/c^2 that fail the BDT selection. Only the yields and the asymmetries of each component are allowed to vary in the fits, which are performed separately in each $m(\mu^+\mu^-)$ region. The resulting efficiency-weighted yields are reported in Table I, together with the measured signal asymmetries. Figure 2 shows the $m(h^+h^-\mu^+\mu^-)$ distribution of the efficiency-weighted candidates integrated in $m(\mu^+\mu^-)$, with the fit projection overlaid.

The following sources of systematic uncertainties affect the measured asymmetries: accuracy of the mass model used in the fit, accuracy of the phase-space-dependent efficiency, neglected asymmetric angular efficiencies and finite resolution on angular variables (affecting only $A_{\rm FB}$ and $A_{2\phi}$); neglected background from D^{*+} candidates made up of correctly reconstructed D^0 candidates paired with unrelated soft pions (affecting only A_{CP} and $A_{\rm FB}$); accuracy of the correction for the nuisance charge asymmetries and neglected backgrounds from D^{*+} candidates originating

TABLE I. Efficiency-weighted yields and measured signal asymmetries for (top) $D^0 \to \pi^+\pi^-\mu^+\mu^-$ and (bottom) $D^0 \to K^+K^-\mu^+\mu^-$ decays in the dimuon-mass regions. For the asymmetries the first uncertainty is statistical and the second systematic. Measurements are reported only in regions where a significant signal was previously observed [12]. The sum of the yields in the dimuon-mass regions is not expected to match the yield of the full range, because the latter includes also the regions where no yields are reported.

	Efficiency-weighted yields			Signal asymmetries		
$m(\mu^+\mu^-)$ [MeV/c^2]	Signal	Misidentified background	Combinatorial background	$A_{\rm FB}$ [%]	$A_{2\phi}$ [%]	A_{CP} [%]
			$D^0 \to \pi^+\pi^-\mu^+\mu^-$			
<525	90 ± 17	233 ± 25	108 ± 22	$2 \pm 20 \pm 2$	$-28 \pm 20 \pm 2$	$17 \pm 20 \pm 2$
525–565	...	...	...	...	...	...
565–780	326 ± 23	253 ± 24	145 ± 21	$8.1 \pm 7.1 \pm 0.7$	$7.4 \pm 7.1 \pm 0.7$	$-12.9 \pm 7.1 \pm 0.7$
780–950	141 ± 14	159 ± 15	89 ± 14	$7 \pm 10 \pm 1$	$-14 \pm 10 \pm 1$	$17 \pm 10 \pm 1$
950–1020	244 ± 16	63 ± 13	43 ± 9	$3.1 \pm 6.5 \pm 0.6$	$1.2 \pm 6.4 \pm 0.5$	$7.5 \pm 6.5 \pm 0.7$
1020–1100	258 ± 14	33 ± 9	44 ± 9	$0.9 \pm 5.6 \pm 0.7$	$1.4 \pm 5.5 \pm 0.6$	$9.9 \pm 5.5 \pm 0.7$
>1100	...	...	...	...	...	...
Full range	1083 ± 41	827 ± 42	579 ± 39	$3.3 \pm 3.7 \pm 0.6$	$-0.6 \pm 3.7 \pm 0.6$	$4.9 \pm 3.8 \pm 0.7$
			$D^0 \to K^+K^-\mu^+\mu^-$			
<525	32 ± 8	5 ± 13	124 ± 20	$13 \pm 26 \pm 4$	$9 \pm 26 \pm 3$	$-33 \pm 26 \pm 4$
525–565	...	...	...	...	...	...
>565	74 ± 9	39 ± 7	48 ± 8	$1 \pm 12 \pm 1$	$22 \pm 12 \pm 1$	$13 \pm 12 \pm 1$
Full range	110 ± 13	49 ± 12	181 ± 19	$0 \pm 11 \pm 2$	$9 \pm 11 \pm 1$	$0 \pm 11 \pm 2$

from b-hadron decays (affecting only A_{CP}). The leading systematic uncertainties are due to the accuracy of the efficiency correction, for all asymmetries; to possible asymmetric efficiencies as a function of $\cos\theta_\mu$ and $\sin 2\phi$, for $A_{\rm FB}$ and $A_{2\phi}$, respectively; and to the uncertainty on the nuisance charge asymmetry, for A_{CP}. The total systematic uncertainties amount to less than 20% of the statistical uncertainties for both decay modes and all dimuon-mass regions (Table I).

The analysis is repeated on statistically independent data subsets chosen according to criteria likely to reveal biases from specific instrumental effects. These criteria include the data-taking year, the magnetic-field orientation, the number of primary vertices in the event, the per-event track multiplicity, the trigger classification, the D^{*+} transverse momentum and the impact parameter of the D^0 candidate with respect to the primary vertex. The resulting variations of the measured asymmetries are consistent with statistical fluctuations, with p values between 3% and 95% and without deviations from a flat distribution.

In summary, measurements of angular and CP asymmetries in $D^0 \to \pi^+\pi^-\mu^+\mu^-$ and $D^0 \to K^+K^-\mu^+\mu^-$ decays are performed using the proton-proton collision data collected with the LHCb experiment between 2011 and 2016. This is the first time such measurements are performed with rare decays of charm hadrons. The asymmetries are measured both integrated and as a function of dimuon mass. The integrated asymmetries are

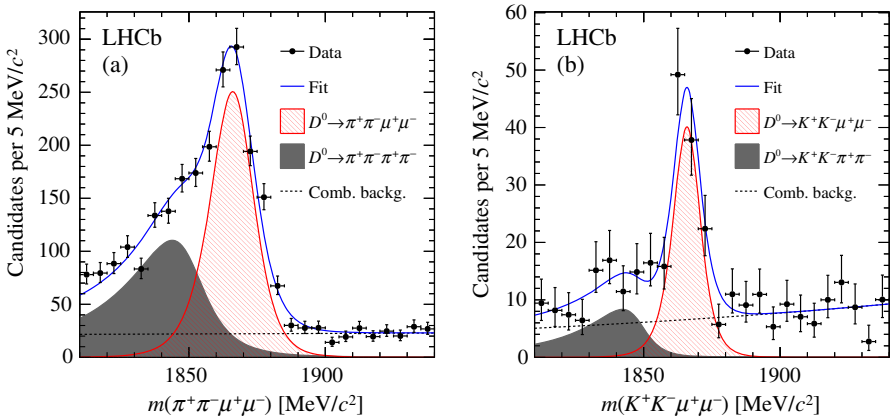

FIG. 2. Distribution of $m(h^+h^-\mu^+\mu^-)$ for (a) $D^0 \to \pi^+\pi^-\mu^+\mu^-$ and (b) $D^0 \to K^+K^-\mu^+\mu^-$ efficiency-weighted candidates, with fit projections overlaid.

$$A_{\rm FB}(D^0 \to \pi^+\pi^-\mu^+\mu^-) = (3.3 \pm 3.7 \pm 0.6)\%,$$
$$A_{2\phi}(D^0 \to \pi^+\pi^-\mu^+\mu^-) = (-0.6 \pm 3.7 \pm 0.6)\%,$$
$$A_{CP}(D^0 \to \pi^+\pi^-\mu^+\mu^-) = (4.9 \pm 3.8 \pm 0.7)\%,$$
$$A_{\rm FB}(D^0 \to K^+K^-\mu^+\mu^-) = (0 \pm 11 \pm 2)\%,$$
$$A_{2\phi}(D^0 \to K^+K^-\mu^+\mu^-) = (9 \pm 11 \pm 1)\%,$$
$$A_{CP}(D^0 \to K^+K^-\mu^+\mu^-) = (0 \pm 11 \pm 2)\%,$$

where the first uncertainty is statistical and the second systematic. These measurements, as well as the asymmetries in each dimuon-mass region, are consistent with zero and will help constrain scenarios of physics beyond the SM [4–8,10,11].

We express our gratitude to our colleagues in the CERN accelerator departments for the excellent performance of the LHC. We thank the technical and administrative staff at the LHCb institutes. We acknowledge support from CERN and from the national agencies: CAPES, CNPq, FAPERJ and FINEP (Brazil); MOST and NSFC (China); CNRS/IN2P3 (France); BMBF, DFG and MPG (Germany); INFN (Italy); NWO (Netherlands); MNiSW and NCN (Poland); MEN/IFA (Romania); MinES and FASO (Russia); MinECo (Spain); SNSF and SER (Switzerland); NASU (Ukraine); STFC (United Kingdom); NSF (USA). We acknowledge the computing resources that are provided by CERN, IN2P3 (France), KIT and DESY (Germany), INFN (Italy), SURF (Netherlands), PIC (Spain), GridPP (United Kingdom), RRCKI and Yandex LLC (Russia), CSCS (Switzerland), IFIN-HH (Romania), CBPF (Brazil), PL-GRID (Poland) and OSC (USA). We are indebted to the communities behind the multiple open-source software packages on which we depend. Individual groups or members have received support from AvH Foundation (Germany), EPLANET, Marie Skłodowska-Curie Actions and ERC (European Union), ANR, Labex P2IO and OCEVU, and Région Auvergne-Rhône-Alpes (France), Key Research Program of Frontier Sciences of CAS, CAS PIFI, and the Thousand Talents Program (China), RFBR, RSF and Yandex LLC (Russia), GVA, XuntaGal and GENCAT (Spain), Herchel Smith Fund, the Royal Society, the English-Speaking Union and the Leverhulme Trust (United Kingdom).

[1] S. L. Glashow, J. Iliopoulos, and L. Maiani, Weak interactions with lepton-hadron symmetry, Phys. Rev. D **2**, 1285 (1970).
[2] A. Paul, I. I. Bigi, and S. Recksiegel, On $D \to X_u \ell^+\ell^-$ within the Standard Model and frameworks like the littlest Higgs model with T parity, Phys. Rev. D **83**, 114006 (2011).
[3] S. Fajfer, N. Košnik, and S. Prelovšek, Updated constraints on new physics in rare charm decays, Phys. Rev. D **76**, 074010 (2007).
[4] L. Cappiello, O. Catà, and G. D'Ambrosio, Standard model prediction and new physics tests for $D^0 \to h_1^+ h_2^- \ell^+\ell^-$ ($h = \pi$, K; $\ell = e$, μ), J. High Energy Phys. 04 (2013) 135.
[5] S. de Boer and G. Hiller, Null tests from angular distributions in $D \to P_1 P_2 l^+ l^-$, $l = e$, μ decays on and off peak, arXiv:1805.08516 [Phys. Rev. D (to be published)].
[6] S. Fajfer and S. Prelovšek, Effects of littlest Higgs model in rare D meson decays, Phys. Rev. D **73**, 054026 (2006).
[7] I. I. Bigi and A. Paul, On *CP* asymmetries in two-, three- and four-body D decays, J. High Energy Phys. 03 (2012) 021.
[8] A. Paul, A. de la Puente, and I. I. Bigi, Manifestations of warped extra dimension in rare charm decays and asymmetries, Phys. Rev. D **90**, 014035 (2014).
[9] S. Fajfer and N. Košnik, Resonance catalyzed *CP* asymmetries in $D \to P\ell^+\ell^-$, Phys. Rev. D **87**, 054026 (2013).
[10] S. Fajfer and N. Košnik, Prospects of discovering new physics in rare charm decays, Eur. Phys. J. C **75**, 567 (2015).
[11] S. de Boer and G. Hiller, Flavor and new physics opportunities with rare charm decays into leptons, Phys. Rev. D **93**, 074001 (2016).
[12] R. Aaij *et al.* (LHCb Collaboration), Observation of D^0 Meson Decays to $\pi^+\pi^-\mu^+\mu^-$ and $K^+K^-\mu^+\mu^-$ Final States, Phys. Rev. Lett. **119**, 181805 (2017).
[13] A. A. Alves Jr. *et al.* (LHCb Collaboration), The LHCb detector at the LHC, J. Instrum. **3**, S08005 (2008).
[14] R. Aaij *et al.* (LHCb Collaboration), LHCb detector performance, Int. J. Mod. Phys. A **30**, 1530022 (2015).
[15] R. Aaij *et al.*, The LHCb trigger and its performance in 2011, J. Instrum. **8**, P04022 (2013).
[16] R. Aaij *et al.* (LHCb Collaboration), Evidence for *CP* Violation in Time-Integrated $D^0 \to h^-h^+$ Decay Rates, Phys. Rev. Lett. **108**, 111602 (2012).
[17] L. Breiman, J. H. Friedman, R. A. Olshen, and C. J. Stone, *Classification and Regression Trees* (Wadsworth International Group, Belmont, California, 1984).
[18] B. P. Roe, H.-J. Yang, J. Zhu, Y. Liu, I. Stancu, and G. McGregor, Boosted decision trees as an alternative to artificial neural networks for particle identification, Nucl. Instrum. Methods Phys. Res., Sect. A **543**, 577 (2005).
[19] A. Hoecker *et al.*, TMVA—Toolkit for Multivariate Data Analysis, Proc. Sci., ACAT (**2007**) 040 [arXiv:physics/0703039].
[20] I. Belyaev *et al.*, Handling of the generation of primary events in Gauss, the LHCb simulation framework, J. Phys. Conf. Ser. **331**, 032047 (2011).
[21] M. Clemencic, G. Corti, S. Easo, C. R. Jones, S. Miglioranzi, M. Pappagallo, and P. Robbe, The LHCb simulation application, Gauss: Design, evolution and experience, J. Phys. Conf. Ser. **331**, 032023 (2011).
[22] F. Archilli *et al.*, Performance of the muon identification at LHCb, J. Instrum. **8**, P10020 (2013).
[23] R. Aaij *et al.*, Selection and processing of calibration samples to measure the particle identification performance of the LHCb experiment in Run 2, arXiv:1803.00824.
[24] B. Viaud, On the potential of multivariate techniques for the determination of multidimensional efficiencies, Eur. Phys. J. Plus **131**, 191 (2016).
[25] R. Aaij *et al.* (LHCb Collaboration), Measurement of *CP* asymmetry in $D^0 \to K^-K^+$ and $D^0 \to \pi^-\pi^+$ decays, J. High Energy Phys. 07 (2014) 041.
[26] N. L. Johnson, Systems of frequency curves generated by methods of translation, Biometrika **36**, 149 (1949).

R. Aaij,[27] B. Adeva,[41] M. Adinolfi,[48] C. A. Aidala,[73] Z. Ajaltouni,[5] S. Akar,[59] P. Albicocco,[18] J. Albrecht,[10] F. Alessio,[42] M. Alexander,[53] A. Alfonso Albero,[40] S. Ali,[27] G. Alkhazov,[33] P. Alvarez Cartelle,[55] A. A. Alves Jr,[41] S. Amato,[2] S. Amerio,[23] Y. Amhis,[7] L. An,[3] L. Anderlini,[17] G. Andreassi,[43] M. Andreotti,[16,g] J. E. Andrews,[60] R. B. Appleby,[56] F. Archilli,[27] P. d'Argent,[12] J. Arnau Romeu,[6] A. Artamonov,[39] M. Artuso,[61] K. Arzymatov,[37] E. Aslanides,[6] M. Atzeni,[44] B. Audurier,[22] S. Bachmann,[12] J. J. Back,[50] S. Baker,[55] V. Balagura,[7,b] W. Baldini,[16] A. Baranov,[37] R. J. Barlow,[56] S. Barsuk,[7] W. Barter,[56] F. Baryshnikov,[70] V. Batozskaya,[31] B. Batsukh,[61] V. Battista,[43] A. Bay,[43] J. Beddow,[53] F. Bedeschi,[24] I. Bediaga,[1] A. Beiter,[61] L. J. Bel,[27] N. Beliy,[63] V. Bellee,[43] N. Belloli,[20,i] K. Belous,[39] I. Belyaev,[34,42] E. Ben-Haim,[8] G. Bencivenni,[18] S. Benson,[27] S. Beranek,[9] A. Berezhnoy,[35] R. Bernet,[44] D. Berninghoff,[12] E. Bertholet,[8] A. Bertolin,[23] C. Betancourt,[44] F. Betti,[15,42] M. O. Bettler,[49] M. van Beuzekom,[27] Ia. Bezshyiko,[44] S. Bhasin,[48] J. Bhom,[29] S. Bifani,[47] P. Billoir,[8] A. Birnkraut,[10] A. Bizzeti,[17,u] M. Bjørn,[57] M. P. Blago,[42] T. Blake,[50] F. Blanc,[43] S. Blusk,[61] D. Bobulska,[53] V. Bocci,[26] O. Boente Garcia,[41] T. Boettcher,[58] A. Bondar,[38,w] N. Bondar,[33] S. Borghi,[56,42] M. Borisyak,[37] M. Borsato,[41] F. Bossu,[7] M. Boubdir,[9] T. J. V. Bowcock,[54] C. Bozzi,[16,42] S. Braun,[12] M. Brodski,[42] J. Brodzicka,[29] A. Brossa Gonzalo,[50] D. Brundu,[22] E. Buchanan,[48] A. Buonaura,[44] C. Burr,[56] A. Bursche,[22] J. Buytaert,[42] W. Byczynski,[42] S. Cadeddu,[22] H. Cai,[64] R. Calabrese,[16,g] R. Calladine,[47] M. Calvi,[20,i] M. Calvo Gomez,[40,m] A. Camboni,[40,m] P. Campana,[18] D. H. Campora Perez,[42] L. Capriotti,[56] A. Carbone,[15,e] G. Carboni,[25] R. Cardinale,[19,h] A. Cardini,[22] P. Carniti,[20,i] L. Carson,[52] K. Carvalho Akiba,[2] G. Casse,[54] L. Cassina,[20] M. Cattaneo,[42] G. Cavallero,[19,h] R. Cenci,[24,p] D. Chamont,[7] M. G. Chapman,[48] M. Charles,[8] Ph. Charpentier,[42] G. Chatzikonstantinidis,[47] M. Chefdeville,[4] V. Chekalina,[37] C. Chen,[3] S. Chen,[22] S.-G. Chitic,[42] V. Chobanova,[41] M. Chrzaszcz,[42] A. Chubykin,[33] P. Ciambrone,[18] X. Cid Vidal,[41] G. Ciezarek,[42] P. E. L. Clarke,[52] M. Clemencic,[42] H. V. Cliff,[49] J. Closier,[42] V. Coco,[42] J. A. B. Coelho,[7] J. Cogan,[6] E. Cogneras,[5] L. Cojocariu,[32] P. Collins,[42] T. Colombo,[42] A. Comerma-Montells,[12] A. Contu,[22] G. Coombs,[42] S. Coquereau,[40] G. Corti,[42] M. Corvo,[16,g] C. M. Costa Sobral,[50] B. Couturier,[42] G. A. Cowan,[52] D. C. Craik,[58] A. Crocombe,[50] M. Cruz Torres,[1] R. Currie,[52] C. D'Ambrosio,[42] F. Da Cunha Marinho,[2] C. L. Da Silva,[74] E. Dall'Occo,[27] J. Dalseno,[48] A. Danilina,[34] A. Davis,[3] O. De Aguiar Francisco,[42] K. De Bruyn,[42] S. De Capua,[56] M. De Cian,[43] J. M. De Miranda,[1] L. De Paula,[2] M. De Serio,[14,d] P. De Simone,[18] C. T. Dean,[53] D. Decamp,[4] L. Del Buono,[8] B. Delaney,[49] H.-P. Dembinski,[11] M. Demmer,[10] A. Dendek,[30] D. Derkach,[37] O. Deschamps,[5] F. Desse,[7] F. Dettori,[54] B. Dey,[65] A. Di Canto,[42] P. Di Nezza,[18] S. Didenko,[70] H. Dijkstra,[42] F. Dordei,[42] M. Dorigo,[42,y] A. Dosil Suárez,[41] L. Douglas,[53] A. Dovbnya,[45] K. Dreimanis,[54] L. Dufour,[27] G. Dujany,[8] P. Durante,[42] J. M. Durham,[74] D. Dutta,[56] R. Dzhelyadin,[39] M. Dziewiecki,[12] A. Dziurda,[29] A. Dzyuba,[33] S. Easo,[51] U. Egede,[55] V. Egorychev,[34] S. Eidelman,[38,w] S. Eisenhardt,[52] U. Eitschberger,[10] R. Ekelhof,[10] L. Eklund,[53] S. Ely,[61] A. Ene,[32] S. Escher,[9] S. Esen,[27] T. Evans,[59] A. Falabella,[15] N. Farley,[47] S. Farry,[54] D. Fazzini,[20,42,i] L. Federici,[25] P. Fernandez Declara,[42] A. Fernandez Prieto,[41] F. Ferrari,[15] L. Ferreira Lopes,[43] F. Ferreira Rodrigues,[2] M. Ferro-Luzzi,[42] S. Filippov,[36] R. A. Fini,[14] M. Fiorini,[16,g] M. Firlej,[30] C. Fitzpatrick,[43] T. Fiutowski,[30] F. Fleuret,[7,b] M. Fontana,[22,42] F. Fontanelli,[19,h] R. Forty,[42] V. Franco Lima,[54] M. Frank,[42] C. Frei,[42] J. Fu,[21,q] W. Funk,[42] C. Färber,[42] M. Féo Pereira Rivello Carvalho,[27] E. Gabriel,[52] A. Gallas Torreira,[41] D. Galli,[15,e] S. Gallorini,[23] S. Gambetta,[52] Y. Gan,[3] M. Gandelman,[2] P. Gandini,[21] Y. Gao,[3] L. M. Garcia Martin,[72] B. Garcia Plana,[41] J. García Pardiñas,[44] J. Garra Tico,[49] L. Garrido,[40] D. Gascon,[40] C. Gaspar,[42] L. Gavardi,[10] G. Gazzoni,[5] D. Gerick,[12] E. Gersabeck,[56] M. Gersabeck,[56] T. Gershon,[50] D. Gerstel,[6] Ph. Ghez,[4] S. Gianì,[43] V. Gibson,[49] O. G. Girard,[43] L. Giubega,[32] K. Gizdov,[52] V. V. Gligorov,[8] D. Golubkov,[34] A. Golutvin,[55,70] A. Gomes,[1,a] I. V. Gorelov,[35] C. Gotti,[20,i] E. Govorkova,[27] J. P. Grabowski,[12] R. Graciani Diaz,[40] L. A. Granado Cardoso,[42] E. Graugés,[40] E. Graverini,[44] G. Graziani,[17] A. Grecu,[32] R. Greim,[27] P. Griffith,[22] L. Grillo,[56] L. Gruber,[42] B. R. Gruberg Cazon,[57] O. Grünberg,[67] C. Gu,[3] E. Gushchin,[36] Yu. Guz,[39,42] T. Gys,[42] C. Göbel,[62] T. Hadavizadeh,[57] C. Hadjivasiliou,[5] G. Haefeli,[43] C. Haen,[42] S. C. Haines,[49] B. Hamilton,[60] X. Han,[12] T. H. Hancock,[57] S. Hansmann-Menzemer,[12] N. Harnew,[57] S. T. Harnew,[48] T. Harrison,[54] C. Hasse,[42] M. Hatch,[42] J. He,[63] M. Hecker,[55] K. Heinicke,[10] A. Heister,[10] K. Hennessy,[54] L. Henry,[72] E. van Herwijnen,[42] M. Heß,[67] A. Hicheur,[2] R. Hidalgo Charman,[56] D. Hill,[57] M. Hilton,[56] P. H. Hopchev,[43] W. Hu,[65] W. Huang,[63] Z. C. Huard,[59] W. Hulsbergen,[27] T. Humair,[55] M. Hushchyn,[37] D. Hutchcroft,[54] D. Hynds,[27] P. Ibis,[10] M. Idzik,[30] P. Ilten,[47] K. Ivshin,[33] R. Jacobsson,[42] J. Jalocha,[57] E. Jans,[27] A. Jawahery,[60] F. Jiang,[3] M. John,[57] D. Johnson,[42] C. R. Jones,[49] C. Joram,[42] B. Jost,[42] N. Jurik,[57] S. Kandybei,[45] M. Karacson,[42] J. M. Kariuki,[48] S. Karodia,[53] N. Kazeev,[37] M. Kecke,[12] F. Keizer,[49] M. Kelsey,[61] M. Kenzie,[49] T. Ketel,[28] E. Khairullin,[37] B. Khanji,[12] C. Khurewathanakul,[43] K. E. Kim,[61] T. Kirn,[9] S. Klaver,[18] K. Klimaszewski,[31] T. Klimkovich,[11] S. Koliiev,[46] M. Kolpin,[12] R. Kopecna,[12] P. Koppenburg,[27] I. Kostiuk,[27] S. Kotriakhova,[33] M. Kozeiha,[5] L. Kravchuk,[36] M. Kreps,[50] F. Kress,[55] P. Krokovny,[38,w] W. Krupa,[30] W. Krzemien,[31]

W. Kucewicz,[29,l] M. Kucharczyk,[29] V. Kudryavtsev,[38,w] A. K. Kuonen,[43] T. Kvaratskheliya,[34,42] D. Lacarrere,[42] G. Lafferty,[56] A. Lai,[22] D. Lancierini,[44] G. Lanfranchi,[18] C. Langenbruch,[9] T. Latham,[50] C. Lazzeroni,[47] R. Le Gac,[6] A. Leflat,[35] J. Lefrançois,[7] R. Lefèvre,[5] F. Lemaitre,[42] O. Leroy,[6] T. Lesiak,[29] B. Leverington,[12] P.-R. Li,[63] T. Li,[3] Z. Li,[61] X. Liang,[61] T. Likhomanenko,[69] R. Lindner,[42] F. Lionetto,[44] V. Lisovskyi,[7] X. Liu,[3] D. Loh,[50] A. Loi,[22] I. Longstaff,[53] J. H. Lopes,[2] G. H. Lovell,[49] D. Lucchesi,[23,o] M. Lucio Martinez,[41] A. Lupato,[23] E. Luppi,[16,g] O. Lupton,[42] A. Lusiani,[24] X. Lyu,[63] F. Machefert,[7] F. Maciuc,[32] V. Macko,[43] P. Mackowiak,[10] S. Maddrell-Mander,[48] O. Maev,[33,42] K. Maguire,[56] D. Maisuzenko,[33] M. W. Majewski,[30] S. Malde,[57] B. Malecki,[29] A. Malinin,[69] T. Maltsev,[38,w] G. Manca,[22,f] G. Mancinelli,[6] D. Marangotto,[21,q] J. Maratas,[5,v] J. F. Marchand,[4] U. Marconi,[15] C. Marin Benito,[7] M. Marinangeli,[43] P. Marino,[43] J. Marks,[12] P. J. Marshall,[54] G. Martellotti,[26] M. Martin,[6] M. Martinelli,[42] D. Martinez Santos,[41] F. Martinez Vidal,[72] A. Massafferri,[1] M. Materok,[9] R. Matev,[42] A. Mathad,[50] Z. Mathe,[42] C. Matteuzzi,[20] A. Mauri,[44] E. Maurice,[7,b] B. Maurin,[43] A. Mazurov,[47] M. McCann,[55,42] A. McNab,[56] R. McNulty,[13] J. V. Mead,[54] B. Meadows,[59] C. Meaux,[6] F. Meier,[10] N. Meinert,[67] D. Melnychuk,[31] M. Merk,[27] A. Merli,[21,q] E. Michielin,[23] D. A. Milanes,[66] E. Millard,[50] M.-N. Minard,[4] L. Minzoni,[16,g] D. S. Mitzel,[12] A. Mogini,[8] J. Molina Rodriguez,[1,z] T. Mombächer,[10] I. A. Monroy,[66] S. Monteil,[5] M. Morandin,[23] G. Morello,[18] M. J. Morello,[24,t] O. Morgunova,[69] J. Moron,[30] A. B. Morris,[6] R. Mountain,[61] F. Muheim,[52] M. Mulder,[27] C. H. Murphy,[57] D. Murray,[56] A. Mödden,[10] D. Müller,[42] J. Müller,[10] K. Müller,[44] V. Müller,[10] P. Naik,[48] T. Nakada,[43] R. Nandakumar,[51] A. Nandi,[57] T. Nanut,[43] I. Nasteva,[2] M. Needham,[52] N. Neri,[21] S. Neubert,[12] N. Neufeld,[42] M. Neuner,[12] T. D. Nguyen,[43] C. Nguyen-Mau,[43,n] S. Nieswand,[9] R. Niet,[10] N. Nikitin,[35] A. Nogay,[69] D. P. O'Hanlon,[15] A. Oblakowska-Mucha,[30] V. Obraztsov,[39] S. Ogilvy,[18] R. Oldeman,[22,f] C. J. G. Onderwater,[68] A. Ossowska,[29] J. M. Otalora Goicochea,[2] P. Owen,[44] A. Oyanguren,[72] P. R. Pais,[43] T. Pajero,[24,t] A. Palano,[14] M. Palutan,[18,42] G. Panshin,[71] A. Papanestis,[51] M. Pappagallo,[52] L. L. Pappalardo,[16,g] W. Parker,[60] C. Parkes,[56] G. Passaleva,[17,42] A. Pastore,[14] M. Patel,[55] C. Patrignani,[15,e] A. Pearce,[42] A. Pellegrino,[27] G. Penso,[26] M. Pepe Altarelli,[42] S. Perazzini,[42] D. Pereima,[34] P. Perret,[5] L. Pescatore,[43] K. Petridis,[48] A. Petrolini,[19,h] A. Petrov,[69] S. Petrucci,[52] M. Petruzzo,[21,q] B. Pietrzyk,[4] G. Pietrzyk,[43] M. Pikies,[29] M. Pili,[57] D. Pinci,[26] J. Pinzino,[42] F. Pisani,[42] A. Piucci,[12] V. Placinta,[32] S. Playfer,[52] J. Plews,[47] M. Plo Casasus,[41] F. Polci,[8] M. Poli Lener,[18] A. Poluektov,[50] N. Polukhina,[70,c] I. Polyakov,[61] E. Polycarpo,[2] G. J. Pomery,[48] S. Ponce,[42] A. Popov,[39] D. Popov,[47,11] S. Poslavskii,[39] C. Potterat,[2] E. Price,[48] J. Prisciandaro,[41] C. Prouve,[48] V. Pugatch,[46] A. Puig Navarro,[44] H. Pullen,[57] G. Punzi,[24,p] W. Qian,[63] J. Qin,[63] R. Quagliani,[8] B. Quintana,[5] B. Rachwal,[30] J. H. Rademacker,[48] M. Rama,[24] M. Ramos Pernas,[41] M. S. Rangel,[2] F. Ratnikov,[37,x] G. Raven,[28] M. Ravonel Salzgeber,[42] M. Reboud,[4] F. Redi,[43] S. Reichert,[10] A. C. dos Reis,[1] F. Reiss,[8] C. Remon Alepuz,[72] Z. Ren,[3] V. Renaudin,[7] S. Ricciardi,[51] S. Richards,[48] K. Rinnert,[54] P. Robbe,[7] A. Robert,[8] A. B. Rodrigues,[43] E. Rodrigues,[59] J. A. Rodriguez Lopez,[66] M. Roehrken,[42] A. Rogozhnikov,[37] S. Roiser,[42] A. Rollings,[57] V. Romanovskiy,[39] A. Romero Vidal,[41] M. Rotondo,[18] M. S. Rudolph,[61] T. Ruf,[42] J. Ruiz Vidal,[72] J. J. Saborido Silva,[41] N. Sagidova,[33] B. Saitta,[22,f] V. Salustino Guimaraes,[62] C. Sanchez Gras,[27] C. Sanchez Mayordomo,[72] B. Sanmartin Sedes,[41] R. Santacesaria,[26] C. Santamarina Rios,[41] M. Santimaria,[18] E. Santovetti,[25,j] G. Sarpis,[56] A. Sarti,[18,k] C. Satriano,[26,s] A. Satta,[25] M. Saur,[63] D. Savrina,[34,35] S. Schael,[9] M. Schellenberg,[10] M. Schiller,[53] H. Schindler,[42] M. Schmelling,[11] T. Schmelzer,[10] B. Schmidt,[42] O. Schneider,[43] A. Schopper,[42] H. F. Schreiner,[59] M. Schubiger,[43] M. H. Schune,[7] R. Schwemmer,[42] B. Sciascia,[18] A. Sciubba,[26,k] A. Semennikov,[34] E. S. Sepulveda,[8] A. Sergi,[47,42] N. Serra,[44] J. Serrano,[6] L. Sestini,[23] A. Seuthe,[10] P. Seyfert,[42] M. Shapkin,[39] Y. Shcheglov,[33,†] T. Shears,[54] L. Shekhtman,[38,w] V. Shevchenko,[69] E. Shmanin,[70] B. G. Siddi,[16] R. Silva Coutinho,[44] L. Silva de Oliveira,[2] G. Simi,[23,o] S. Simone,[14,d] N. Skidmore,[12] T. Skwarnicki,[61] J. G. Smeaton,[49] E. Smith,[9] I. T. Smith,[52] M. Smith,[55] M. Soares,[15] l. Soares Lavra,[1] M. D. Sokoloff,[59] F. J. P. Soler,[53] B. Souza De Paula,[2] B. Spaan,[10] P. Spradlin,[53] F. Stagni,[42] M. Stahl,[12] S. Stahl,[42] P. Stefko,[43] S. Stefkova,[55] O. Steinkamp,[44] S. Stemmle,[12] O. Stenyakin,[39] M. Stepanova,[33] H. Stevens,[10] S. Stone,[61] B. Storaci,[44] S. Stracka,[24,p] M. E. Stramaglia,[43] M. Straticiuc,[32] U. Straumann,[44] S. Strokov,[71] J. Sun,[3] L. Sun,[64] K. Swientek,[30] V. Syropoulos,[28] T. Szumlak,[30] M. Szymanski,[63] S. T'Jampens,[4] Z. Tang,[3] A. Tayduganov,[6] T. Tekampe,[10] G. Tellarini,[16] F. Teubert,[42] E. Thomas,[42] J. van Tilburg,[27] M. J. Tilley,[55] V. Tisserand,[5] M. Tobin,[30] S. Tolk,[42] L. Tomassetti,[16,g] D. Tonelli,[24] D. Y. Tou,[8] R. Tourinho Jadallah Aoude,[1] E. Tournefier,[4] M. Traill,[53] M. T. Tran,[43] A. Trisovic,[49] A. Tsaregorodtsev,[6] G. Tuci,[24] A. Tully,[49] N. Tuning,[27,42] A. Ukleja,[31] A. Usachov,[7] A. Ustyuzhanin,[37] U. Uwer,[12] C. Vacca,[22,f] A. Vagner,[71] V. Vagnoni,[15] A. Valassi,[42] S. Valat,[42] G. Valenti,[15] R. Vazquez Gomez,[42] P. Vazquez Regueiro,[41] S. Vecchi,[16] M. van Veghel,[27] J. J. Velthuis,[48] M. Veltri,[17,r] G. Veneziano,[57] A. Venkateswaran,[61] T. A. Verlage,[9] M. Vernet,[5] M. Veronesi,[27] N. V. Veronika,[13] M. Vesterinen,[57] J. V. Viana Barbosa,[42] D. Vieira,[63] M. Vieites Diaz,[41] H. Viemann,[67] X. Vilasis-Cardona,[40,m] A. Vitkovskiy,[27] M. Vitti,[49] V. Volkov,[35]

A. Vollhardt,[44] B. Voneki,[42] A. Vorobyev,[33] V. Vorobyev,[38,w] J. A. de Vries,[27] C. Vázquez Sierra,[27] R. Waldi,[67] J. Walsh,[24] J. Wang,[61] M. Wang,[3] Y. Wang,[65] Z. Wang,[44] D. R. Ward,[49] H. M. Wark,[54] N. K. Watson,[47] D. Websdale,[55] A. Weiden,[44] C. Weisser,[58] M. Whitehead,[9] J. Wicht,[50] G. Wilkinson,[57] M. Wilkinson,[61] I. Williams,[49] M. R. J. Williams,[56] M. Williams,[58] T. Williams,[47] F. F. Wilson,[51,42] J. Wimberley,[60] M. Winn,[7] J. Wishahi,[10] W. Wislicki,[31] M. Witek,[29] G. Wormser,[7] S. A. Wotton,[49] K. Wyllie,[42] D. Xiao,[65] Y. Xie,[65] A. Xu,[3] M. Xu,[65] Q. Xu,[63] Z. Xu,[3] Z. Xu,[4] Z. Yang,[3] Z. Yang,[60] Y. Yao,[61] L. E. Yeomans,[54] H. Yin,[65] J. Yu,[65,ab] X. Yuan,[61] O. Yushchenko,[39] K. A. Zarebski,[47] M. Zavertyaev,[11,c] D. Zhang,[65] L. Zhang,[3] W. C. Zhang,[3,aa] Y. Zhang,[7] A. Zhelezov,[12] Y. Zheng,[63] X. Zhu,[3] V. Zhukov,[9,35] J. B. Zonneveld,[52] and S. Zucchelli[15]

(LHCb Collaboration)

[1]*Centro Brasileiro de Pesquisas Físicas (CBPF), Rio de Janeiro, Brazil*
[2]*Universidade Federal do Rio de Janeiro (UFRJ), Rio de Janeiro, Brazil*
[3]*Center for High Energy Physics, Tsinghua University, Beijing, China*
[4]*Univ. Grenoble Alpes, Univ. Savoie Mont Blanc, CNRS, IN2P3-LAPP, Annecy, France*
[5]*Clermont Université, Université Blaise Pascal, CNRS/IN2P3, LPC, Clermont-Ferrand, France*
[6]*Aix Marseille Univ, CNRS/IN2P3, CPPM, Marseille, France*
[7]*LAL, Univ. Paris-Sud, CNRS/IN2P3, Université Paris-Saclay, Orsay, France*
[8]*LPNHE, Sorbonne Université, Paris Diderot Sorbonne Paris Cité, CNRS/IN2P3, Paris, France*
[9]*I. Physikalisches Institut, RWTH Aachen University, Aachen, Germany*
[10]*Fakultät Physik, Technische Universität Dortmund, Dortmund, Germany*
[11]*Max-Planck-Institut für Kernphysik (MPIK), Heidelberg, Germany*
[12]*Physikalisches Institut, Ruprecht-Karls-Universität Heidelberg, Heidelberg, Germany*
[13]*School of Physics, University College Dublin, Dublin, Ireland*
[14]*INFN Sezione di Bari, Bari, Italy*
[15]*INFN Sezione di Bologna, Bologna, Italy*
[16]*INFN Sezione di Ferrara, Ferrara, Italy*
[17]*INFN Sezione di Firenze, Firenze, Italy*
[18]*INFN Laboratori Nazionali di Frascati, Frascati, Italy*
[19]*INFN Sezione di Genova, Genova, Italy*
[20]*INFN Sezione di Milano-Bicocca, Milano, Italy*
[21]*INFN Sezione di Milano, Milano, Italy*
[22]*INFN Sezione di Cagliari, Monserrato, Italy*
[23]*INFN Sezione di Padova, Padova, Italy*
[24]*INFN Sezione di Pisa, Pisa, Italy*
[25]*INFN Sezione di Roma Tor Vergata, Roma, Italy*
[26]*INFN Sezione di Roma La Sapienza, Roma, Italy*
[27]*Nikhef National Institute for Subatomic Physics, Amsterdam, Netherlands*
[28]*Nikhef National Institute for Subatomic Physics and VU University Amsterdam, Amsterdam, Netherlands*
[29]*Henryk Niewodniczanski Institute of Nuclear Physics Polish Academy of Sciences, Kraków, Poland*
[30]*AGH - University of Science and Technology, Faculty of Physics and Applied Computer Science, Kraków, Poland*
[31]*National Center for Nuclear Research (NCBJ), Warsaw, Poland*
[32]*Horia Hulubei National Institute of Physics and Nuclear Engineering, Bucharest-Magurele, Romania*
[33]*Petersburg Nuclear Physics Institute (PNPI), Gatchina, Russia*
[34]*Institute of Theoretical and Experimental Physics (ITEP), Moscow, Russia*
[35]*Institute of Nuclear Physics, Moscow State University (SINP MSU), Moscow, Russia*
[36]*Institute for Nuclear Research of the Russian Academy of Sciences (INR RAS), Moscow, Russia*
[37]*Yandex School of Data Analysis, Moscow, Russia*
[38]*Budker Institute of Nuclear Physics (SB RAS), Novosibirsk, Russia*
[39]*Institute for High Energy Physics (IHEP), Protvino, Russia*
[40]*ICCUB, Universitat de Barcelona, Barcelona, Spain*
[41]*Instituto Galego de Física de Altas Enerxías (IGFAE), Universidade de Santiago de Compostela, Santiago de Compostela, Spain*
[42]*European Organization for Nuclear Research (CERN), Geneva, Switzerland*
[43]*Institute of Physics, Ecole Polytechnique Fédérale de Lausanne (EPFL), Lausanne, Switzerland*
[44]*Physik-Institut, Universität Zürich, Zürich, Switzerland*
[45]*NSC Kharkiv Institute of Physics and Technology (NSC KIPT), Kharkiv, Ukraine*

[46]Institute for Nuclear Research of the National Academy of Sciences (KINR), Kyiv, Ukraine
[47]University of Birmingham, Birmingham, United Kingdom
[48]H.H. Wills Physics Laboratory, University of Bristol, Bristol, United Kingdom
[49]Cavendish Laboratory, University of Cambridge, Cambridge, United Kingdom
[50]Department of Physics, University of Warwick, Coventry, United Kingdom
[51]STFC Rutherford Appleton Laboratory, Didcot, United Kingdom
[52]School of Physics and Astronomy, University of Edinburgh, Edinburgh, United Kingdom
[53]School of Physics and Astronomy, University of Glasgow, Glasgow, United Kingdom
[54]Oliver Lodge Laboratory, University of Liverpool, Liverpool, United Kingdom
[55]Imperial College London, London, United Kingdom
[56]School of Physics and Astronomy, University of Manchester, Manchester, United Kingdom
[57]Department of Physics, University of Oxford, Oxford, United Kingdom
[58]Massachusetts Institute of Technology, Cambridge, Massachusetts, USA
[59]University of Cincinnati, Cincinnati, Ohio, USA
[60]University of Maryland, College Park, Maryland, USA
[61]Syracuse University, Syracuse, New York, USA
[62]Pontifícia Universidade Católica do Rio de Janeiro (PUC-Rio), Rio de Janeiro, Brazil
(associated with Universidade Federal do Rio de Janeiro (UFRJ), Rio de Janeiro, Brazil)
[63]University of Chinese Academy of Sciences, Beijing, China
(associated with Center for High Energy Physics, Tsinghua University, Beijing, China)
[64]School of Physics and Technology, Wuhan University, Wuhan, China
(associated with Center for High Energy Physics, Tsinghua University, Beijing, China)
[65]Institute of Particle Physics, Central China Normal University, Wuhan, Hubei, China
(associated with Center for High Energy Physics, Tsinghua University, Beijing, China)
[66]Departamento de Fisica, Universidad Nacional de Colombia, Bogota, Colombia
(associated with LPNHE, Sorbonne Université, Paris Diderot Sorbonne Paris Cité, CNRS/IN2P3, Paris, France)
[67]Institut für Physik, Universität Rostock, Rostock, Germany
(associated with Physikalisches Institut, Ruprecht-Karls-Universität Heidelberg, Heidelberg, Germany)
[68]Van Swinderen Institute, University of Groningen, Groningen, Netherlands
(associated with Nikhef National Institute for Subatomic Physics, Amsterdam, Netherlands)
[69]National Research Centre Kurchatov Institute, Moscow, Russia
[associated with Institute of Theoretical and Experimental Physics (ITEP), Moscow, Russia]
[70]National University of Science and Technology "MISIS", Moscow, Russia
[associated with Institute of Theoretical and Experimental Physics (ITEP), Moscow, Russia]
[71]National Research Tomsk Polytechnic University, Tomsk, Russia
[associated with Institute of Theoretical and Experimental Physics (ITEP), Moscow, Russia]
[72]Instituto de Fisica Corpuscular, Centro Mixto Universidad de Valencia - CSIC, Valencia, Spain
(associated with ICCUB, Universitat de Barcelona, Barcelona, Spain)
[73]University of Michigan, Ann Arbor, USA
(associated with Syracuse University, Syracuse, New York, USA)
[74]Los Alamos National Laboratory (LANL), Los Alamos, USA
(associated with Syracuse University, Syracuse, New York, USA)

[†]Deceased.
[a]Also at Universidade Federal do Triângulo Mineiro (UFTM), Uberaba-MG, Brazil.
[b]Also at Laboratoire Leprince-Ringuet, Palaiseau, France.
[c]Also at P.N. Lebedev Physical Institute, Russian Academy of Science (LPI RAS), Moscow, Russia.
[d]Also at Università di Bari, Bari, Italy.
[e]Also at Università di Bologna, Bologna, Italy.
[f]Also at Università di Cagliari, Cagliari, Italy.
[g]Also at Università di Ferrara, Ferrara, Italy.
[h]Also at Università di Genova, Genova, Italy.
[i]Also at Università di Milano Bicocca, Milano, Italy.
[j]Also at Università di Roma Tor Vergata, Roma, Italy.
[k]Also at Università di Roma La Sapienza, Roma, Italy.
[l]Also at AGH - University of Science and Technology, Faculty of Computer Science, Electronics and Telecommunications, Kraków, Poland.
[m]Also at LIFAELS, La Salle, Universitat Ramon Llull, Barcelona, Spain.

[n]Also at Hanoi University of Science, Hanoi, Vietnam.
[o]Also at Università di Padova, Padova, Italy.
[p]Also at Università di Pisa, Pisa, Italy.
[q]Also at Università degli Studi di Milano, Milano, Italy.
[r]Also at Università di Urbino, Urbino, Italy.
[s]Also at Università della Basilicata, Potenza, Italy.
[t]Also at Scuola Normale Superiore, Pisa, Italy.
[u]Also at Università di Modena e Reggio Emilia, Modena, Italy.
[v]Also at MSU - Iligan Institute of Technology (MSU-IIT), Iligan, Philippines.
[w]Also at Novosibirsk State University, Novosibirsk, Russia.
[x]Also at National Research University Higher School of Economics, Moscow, Russia.
[y]Also at Sezione INFN di Trieste, Trieste, Italy.
[z]Also at Escuela Agrícola Panamericana, San Antonio de Oriente, Honduras.
[aa]Also at School of Physics and Information Technology, Shaanxi Normal University (SNNU), Xi'an, China.
[ab]Also at Physics and Micro Electronic College, Hunan University, Changsha City, China.